analytical chemistry

Article

pubs.acs.org/ac

# Parallel Factor Analysis of 4.2 K Excitation−Emission Matrices for the Direct Determination of Dibenzopyrene Isomers in Coal-Tar Samples with a Cryogenic Fiber-Optic Probe Coupled to a Commercial Spectrofluorimeter

Anthony F. T. Moore,[†] Hector C. Goicoechea,[§] Fernando Barbosa, Jr.,[‡] and Andres D. Campiglia*[,†]

[†]University of Central Florida, Department of Chemistry, 4111 Libra Drive, Physical Sciences Building Room 255, Orlando, Florida 32816-2366, United States

[§]Laboratorio de Desarrollo Analítico y Quimiometría (LADAQ), Cátedra de Química Analítica I, Facultad de Bioquímica y Ciencias Biológicas, Universidad Nacional de Litoral, Santa Fe S3000ZAA, Argentina

[‡]Laboratório de Toxicologia e Essencialidade de Metais, Faculdade de Ciências Farmacêuticas de Ribeirão Preto, Universidade de São Paulo, Avenida do Café s/n, Monte Alegre, 1404903, Ribeirão Preto-SP, Brazil

Supporting Information

**ABSTRACT:** Several studies have shown high concentrations of polycyclic aromatic hydrocarbons (PAHs) in living spaces and soil adjacent to parking lots sealed with coal-tar-based products. Recent attention has been paid to the presence of seven PAHs in coal-tar samples, namely, benz[*a*]anthracene, benzo[*k*]-fluoranthene, benzo[*b*]fluoranthene, benzo[*a*]pyrene, chrysene, dibenz[*a,h*]anthracene, and indeno[*1,2,3-cd*]pyrene, and their association to significant increases in estimated excess lifetime cancer risk for nearby residents. Herein, we present an analytical approach to screen the presence of five highly toxic, high-molecular weight PAHs (HMW-PAHs) in coal-tar samples. These include dibenzo[*a,l*]pyrene, dibenzo[*a,i*]pyrene, dibenzo[*a,e*]pyrene, dibenzo[*a,h*]pyrene, and naphtho[*2,3-a*]-pyrene. Their direct analysis, without chromatographic separation, in a reference coal-tar sample is made possible with the combination of excitation−emission matrices (EEMs) and parallel factor analysis (PARAFAC). EEMs are recorded at 4.2 K with the aid of a cryogenic fiber-optic probe and a commercial spectrofluorimeter. The simplicity of the experimental procedure and the excellent analytical figures of merit demonstrate the screening potential of this environmentally friendly approach for the routine analysis of numerous coal-tar samples.

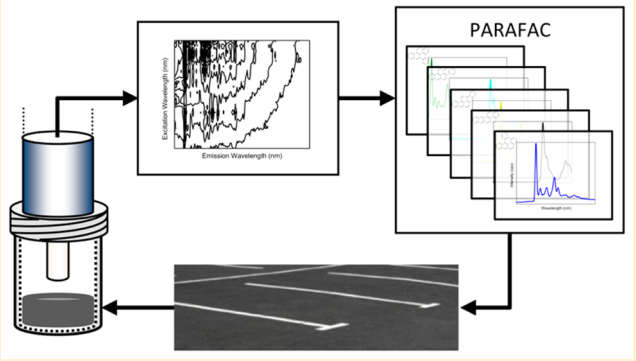


Chemical analysis of polycyclic aromatic hydrocarbons (PAHs) is of great environmental and toxicological importance. Many of them are highly suspect as etiological agents in human cancer.[1−4] Particular attention has been focused on the 16 PAHs included in the U.S. Environmental Protection Agency (EPA) list of priority pollutants.[5] However, a significant portion of the biological activity of PAH-contaminated samples is also attributed to the presence of high-molecular weight (HMW) PAHs, i.e., PAHs with MW ≥ 300.[6−9] Since the carcinogenic properties of HMW-PAHs differ significantly from isomer to isomer, it is important to determine the most toxic isomers even if they are present at much lower concentrations than their less toxic isomers. This is not a trivial task, as many isomers present very similar chromatographic behaviors and virtually identical mass fragmentation patterns.[10] A crucial example is dibenzo[*a,l*]pyrene (DB[*a,l*]P), the most potent carcinogenic PAH known to date.[11−13] Its toxicity is considerably higher than that of benzo[*a*]pyrene, which is the most carcinogenic EPA-PAH. There are several more isomers of dibenzopyrene that are also carcinogenic but not to the extent of DB[*a,l*]P.

A recent trend for the environmental monitoring of PAHs focuses on the development of screening techniques capable to process numerous samples in short analysis time. Screening methods have the potential to prevent unnecessary scrutiny of uncontaminated samples via time-consuming chromatographic procedures, reduce analysis cost, and expedite turnaround time for decision making and remediation purposes. Particularly effective for the direct monitoring, i.e., without chromatographic separation, of EPA-PAHs is the combination of multidimensional fluorescence data with second-order multi-

**Received:** January 12, 2015
**Accepted:** April 22, 2015
**Published:** April 22, 2015





DOI: 10.1021/acs.analchem.5b00147
*Anal. Chem.* 2015, 87, 5232−5239

variate calibration methods. The analyses of phenanthrene and benzo[*k*]fluoranthene in urban runoff water samples,[14] benzo[*a*]pyrene and dibenzo[*a,h*]anthracene in underground, tap, and mineral water samples,[15] and chrysene, benzo[*b*]fluoranthene, benzo[*k*]fluoranthene, and benzo[*a*]anthracene in river water and sludge samples[16] have been reported via room temperature fluorescence excitation−emission matrix (RTF-EEM) spectroscopy combined to either parallel factor analysis (PARAFAC) or unfolded partial least-squares/residual-bilinearization (U-PLS/RBL).

This Article deals with the direct determination of DB[*a,l*]P and four of its isomers, namely, dibenzo[*a,h*]pyrene (DB[*a,h*]P), dibenzo[*a,i*]pyrene (DB[*a,i*]P), dibenzo[*a,e*]pyrene (DB[*a,e*]P), and naphtho[*2,3-a*]pyrene (N[*2,3-a*]P), in a coal-tar standard reference material (NIST SRM 1597a). Coal-tar-based sealcoats are prolific sources of PAHs extensively used all over the world.[17−20] The first determination of DB[*a,l*]P in river sediment samples was reported by Kozin and co-workers using laser-excited Shpol'skii spectrometry.[21,22] Later chromatographic efforts reported its presence in several standard reference materials[23−26] as well as ambient particulate matter from street canyon, a rooftop, and an underground subway station in Stockholm, Sweden.[27] Research in our lab has focused on the determination of HMW-PAHs via laser excited time-resolved Shpol'skii spectroscopy (LETRSS),[10,28−30] which refers to the collection of multidimensional data formats during the lifetime decay of fluorescence emission. Adding the temporal dimension to Shpol'skii spectra provides a particularly selective tool for the determination of structural isomers without previous chromatographic separation. Wavelength−time matrices take advantage of the full dimensionality of fluorescence spectroscopy by combining spectral and lifetime information in a single data format.[31,32] Collection of time-resolved excitation−emission matrices (TREEMs) was made possible with the aid of an in-house instrumental setup consisting of a pulsed tunable dye laser, a pulse delay generator, a spectrograph, and an intensified charge-coupled device. The complications of traditional methodology for low temperature, 77 and 4.2 K, measurements were avoided by using a bifurcated fiber-optic probe (FOP) that delivered the excitation light directly into the frozen matrix. This approach retains the simplicity of dunking the sample into the liquid cryogen for fast and reproducible freezing with no need for an optical Dewar and/or helium cryostat. Frozen samples are prepared in a matter of seconds.[33]

The approach presented here is based on 4.2 K EEMs, Shpol'skii spectroscopy and PARAFAC. We take advantage of the FOP, but we couple it to a commercial spectrofluorimeter. The extent of our literature search revealed no reports on the direct analysis of HMW-PAHs in complex environmental samples via low temperature, steady-state EEM spectroscopy. The broad-band excitation source and the monochromators of the spectrometer facilitate the collection of EEMs throughout a wide range of excitation and emission wavelengths. Lowering the temperature to 4.2 K provides sufficient spectral narrowing for the PARAFAC determination of the five dibenzopyrene isomers in an extremely challenging, complex environmental matrix. The robustness of this approach for screening HMW-PAHs in complex environmental extracts is demonstrated with a straightforward experimental procedure and excellent analytical figures of merit.

## EXPERIMENTAL SECTION

**Instrumentation.** The FOP consisted of one delivery (excitation) and six collection (emission) fibers. All fibers were 2 m long and had a 500 $\mu$m core diameter, silica-clad silica with polyimide buffer coating (Polymicro Technologies, Inc.). The fibers were fed into a 1.2 m long section of copper tubing that provided mechanical support for lowering the probe into the liquid cryogen. At the sample end, the fibers were arranged in a conventional six-around-one configuration with the excitation fiber in the center. At the instrument end, the emission fibers were positioned in a slit configuration. At both ends, vacuum epoxy was used to hold the fibers in place, which were then fed into metal sleeves for mechanical support and polished with a diamond rotating disk. At the sample end, the copper tubing was flared, retaining a phenolic screw cap threaded for a 0.75 mL propylene sample vial.

Fluorescence measurements were carried out with a FluoroMax−P (Horiba Jobin-Yvon) equipped with a 150 W xenon arc source. The 1200 grooves/mm gratings in the single excitation and emission monochromators were blazed at 330 and 500 nm, respectively. Their reciprocal linear dispersion was equal to 4.25 nm/mm. The uncooled photomultiplier tube (Hamamatsu, Model R928) detector was operated in the photon-counting mode. The excitation fiber and the emission fiber bundle of the FOP were coupled to the sample compartment of the spectrofluorimeter with the aid of a commercial fiber-optic mount (F-3000, Horiba Jobin-Yvon) that optimized collection efficiency via two concave mirrors.[34] Position alignment of each end of the FOP with the respective focusing mirror was facilitated by commercially available adapters (Horiba Jobin-Yvon). Commercial software (DataMax version 2.20, Horiba Jobin-Yvon) was used for automated scanning and fluorescence data acquisition.

**Reagents.** All chemicals were analytical-reagent grade and used without further purification. DB[*a,l*]P, DB[*a,e*]P, DB[*a,h*]P, and DB[*a,i*]P were purchased from Accustandard at 100% purity. N[*2,3-a*]P was purchased from Sigma-Aldrich. *n*-Octane (extra pure, 99+%) was acquired from Fischer Scientific. The standard reference material (NIST SRM 1597a) was obtained from the National Institute of Standards and Technology (NIST).

**Solution Preparation for Calibration, Validation, and Coal-Tar Test Samples.** Stock solutions of PAHs were kept in the dark at 4 °C. Possible PAH degradation was monitored via room temperature fluorescence spectroscopy. For each PAH, calibration samples were prepared by serial dilution of stock solutions prior to data collection. A validation sample is a synthetic mixture of the five HMW-PAHs. Twelve validation samples were devised on the basis of a factorial experimental design, consisting of three concentration levels for each of the five HMW-PAHs. Each level is represented by a concentration near the lower limit, near the median concentration, and near the upper limit of the linear dynamic range of the PAH. For the validation samples, appropriate volumes of PAH stock solutions were combined and diluted to the appropriate volume with *n*-octane. Similarly, for the spiked coal-tar test samples, appropriate volumes of the PAH stock solutions and of the coal tar extract were combined and diluted with *n*-octane.

**Fluorescence Measurements.** Room temperature fluorescence measurements were carried out by pouring liquid solutions into a standard quartz cuvette (1 cm path length). FOP measurements were made as follows: after microliter



DOI: 10.1021/acs.analchem.5b00147
*Anal. Chem.* 2015, 87, 5232−5239

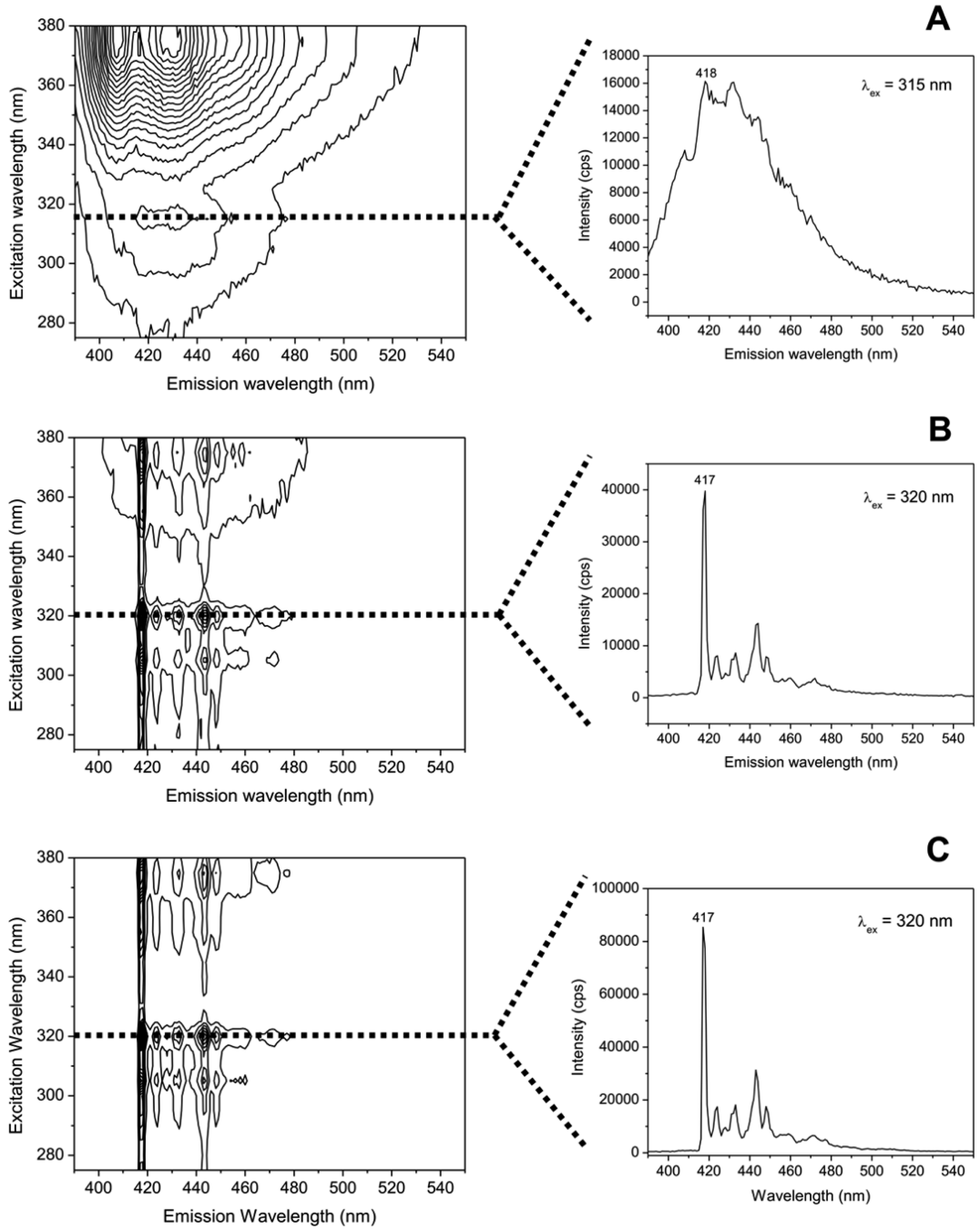


**Figure 1.** Spectral features of DB[*a*,*l*]P at (A) room temperature, (B) 77 K, and (C) 4.2 K in *n*-octane. Spectra were recorded with the aid of a cryogenic fiber-optic probe. Excitation/emission band-passes were as follows: (A) 3/3 nm, (B) 1/1 nm, and (C) 1/1 nm.

volumes (100−750 μL) of undegassed sample solution were pipetted into the sample vial, the sample vial was secured to the sample end of the copper tubing, and the tip of the FOP was positioned at a constant depth below the solution surface. Sample freezing was accomplished by lowering the sample vial into the liquid cryogen. Liquid nitrogen and liquid helium were held in two separate Dewar containers with 5 and 60 L storage capacity, respectively. The 60 L liquid helium volume would typically last for 3 weeks of daily use, averaging 15−20 samples per day. At both 77 and 4.2 K, complete sample freezing took less than 90 s. The ∼1 min probe cleanup procedure involved removing the sample vial from the cryogen container, melting the frozen matrix, warming the resulting solution to approximately room temperature with a heat gun, rinsing the probe with *n*-alkane, and drying it with warm air from the heat gun. The entire freeze, thaw, and cleanup cycle took less than 5 min.

**Software.** All calculations were done using MATLAB 7.10 (MATLAB 7.10 (2010) The MathWorks Inc., Natick, Massachusetts, USA). PARAFAC was applied with the MVC2 graphical user interface written in MATLAB by Olivieri et al.[35] and available on the Internet.[36]

## RESULTS AND DISCUSSION

**Spectral Features of Dibenzopyrene Isomers in *n*-Octane at 77 K and 4.2 K.** Previous research in our lab



DOI: 10.1021/acs.analchem.5b00147
*Anal. Chem.* 2015, 87, 5232−5239

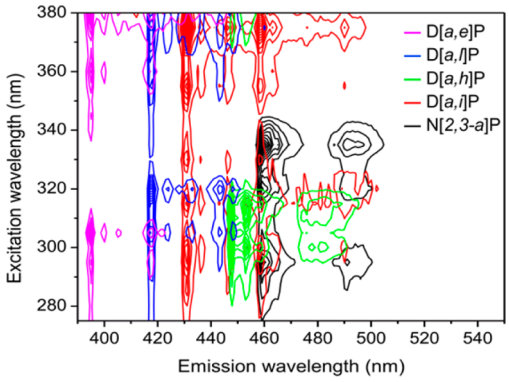


**Figure 2.** Superposition of 4.2 K excitation−emission matrices recorded from calibration sample solutions of (A) 200 ng·mL$^{-1}$ DB[*a,l*]P; (B) 300 ng·mL$^{-1}$ DB[*a,i*]P; (C) 200 ng·mL$^{-1}$ DB[*a,h*]P; (D) 400 ng·mL$^{-1}$ DB[*a,e*]P; and (E) 250 ng·mL$^{-1}$ N[2,3-*a*]P in *n*-octane. All EEMs were recorded with the cryogenic fiber-optic probe using a 1 nm/1 nm excitation/emission band-pass.

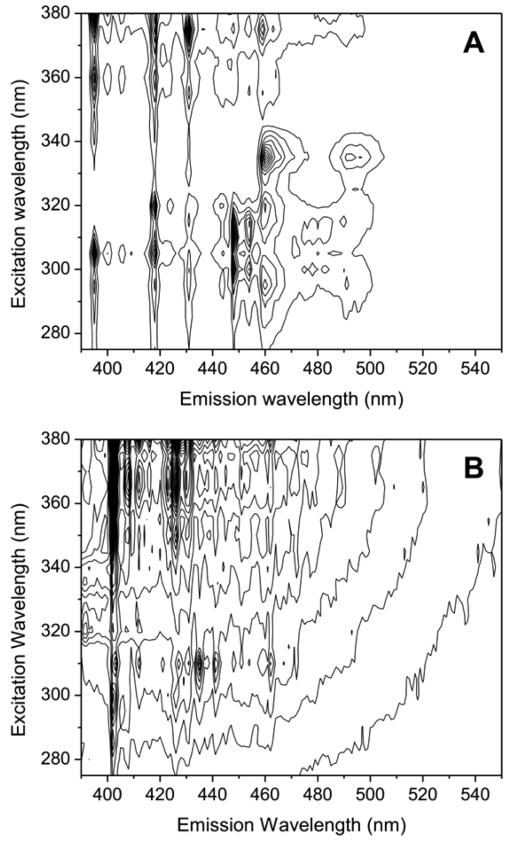


**Figure 3.** 4.2 K excitation−emission matrix of (A) a validation sample containing 180 ng·mL$^{-1}$ DB[*a,l*]P, 180 ng·mL$^{-1}$ DB[*a,i*]P, 180 ng·mL$^{-1}$ DB[*a,h*]P, 450 ng·mL$^{-1}$ DB[*a,e*]P, and 260 ng·mL$^{-1}$ N[2,3-*a*]P in *n*-octane; (B) a 1:375 dilution of NIST SRM 1597a in *n*-octane. Both EEMs were recorded with the cryogenic fiber-optic probe using a 1 nm/1 nm excitation/emission band-pass.

investigated the 4.2 K spectral features and fluorescence lifetimes of DB[*a,l*]P, DB[*a,e*]P, DB[*a,h*]P, DB[*a,i*]P, and N[2,3-*a*]P in three Shpol'skii matrixes, namely, *n*-hexane, *n*-heptane, and *n*-octane. The best spectral narrowing was obtained with *n*-octane,[28−30] which is the solvent selected here for all current studies. The excitation and emission band-pass for the collection of EEMs were set to an acceptable compromise between spectral resolution and signal-to-noise ratio at the parts-per-billion concentration levels. The excitation (275−380 nm) and emission (390−550 nm) wavelength ranges were common to the five studied isomers and gathered most of their spectral signatures. The excitation and emission monochromators were stepped at 5 and 1 nm increments, respectively. These settings provided individual EEMs with 22 emission spectra and 161 data points per emission spectrum. A long-pass filter with 50% transmittance at approximately 320 nm (cutoff wavelength) was used in all cases to minimize instrumental artifacts such as scattered radiation and second-order emission.

**Table 1. 4.2 K Analytical Figures of Merit at Excitation and Emission Wavelengths Free from Spectral Overlapping of Other Isomers**[a]

| PAH | $\lambda_{exc}/\lambda_{em}$ (nm)[b] | LDR (ng·mL$^{-1}$)[c] | $R^2$[d] | LOD (ng·mL$^{-1}$)[e] |
|---|---|---|---|---|
| DB[*a,l*]P | 320/417 | 1.61−400 | 0.9805 | 1.61 |
| DB[*a,e*]P | 305/395 | 4.76−800 | 0.9991 | 4.76 |
| DB[*a,i*]P | 355/430 | 1.63−400 | 0.9934 | 1.63 |
| DB[*a,h*]P | 300/483 | 3.00−300 | 0.9899 | 3.00 |
| N[2,3-*a*]P | 335/491 | 2.32−500 | 0.9915 | 2.32 |

[a]Fluorescence was recorded using an excitation and emission band-pass of 1 nm. [b]Excitation and emission wavelengths. [c]LDR = linear dynamic range in ng·mL$^{-1}$ extending from the limit of detection (LOD) to an arbitrarily chosen upper linear concentration. [d]$R^2$ = coefficient of determination of the calibration curve. [e]Limit of detection calculated as $3 \times S_B/m$, where $S_B$ is the standard deviation of three blank measurements and $m$ is the slope of the calibration curve.

Figure 1 compares the spectral features of DB[*a,l*]P at room temperature, 77 K, and 4.2 K. A 3/3 nm excitation/emission band-pass was needed to obtain an acceptable signal-to-noise ratio at room temperature. The low temperature data was recorded using a 1/1 nm excitation/emission band-pass. The spectral features of DB[*a,l*]P at both 77 and 4.2 K show the quasi-line structure often observed from Shpol'skii systems. Table S1, Supporting Information, summarizes the fluorescence intensities and the full-width at half maxima (fwhm) of the studied isomers at low temperature. Lowering the temperature from 77 to 4.2 K enhanced the fluorescence intensities of the five studied isomers. With the exception of DB[*a,i*]P, all the other isomers presented slightly narrower fwhm at 4.2 K. The fwhm of DB[*a,i*]P was statistically equivalent ($N_1 = N_2 = 3$; $\alpha = 0.05$)[37] at both temperatures. The worst (largest) 4.2 K fwhm was observed from N[2,3-*a*]P. This is probably due to the poorer guest−host compatibility of N[2,3-*a*]P in *n*-octane.

**EEMs and Analytical Figures of Merit of Dibenzopyrene Isomers at 77 and 4.2 K.** Table S2, Supporting Information, compares the analytical figures of merit (AFOM) of the five dibenzopyrene isomers at room temperature, 77 K, and 4.2 K. Fluorescence intensities were extracted from the EEMs at the maximum excitation and emission wavelengths of each PAH. The linear dynamic ranges (LDR) are based on the average intensities ($N = 3$) of at least five PAH concentrations. No efforts were made to reach the upper concentration limits of the calibration curves. The correlation coefficients close to unity demonstrate linear correlations in all cases. The limits of detection (LODs) were calculated as $3 \times S_B/m$, where $S_B$ is the standard deviation of the average blank signal extracted from three EEMs and $m$ is the slope of the calibration curve. The blank signals were measured at the maximum excitation and


DOI: 10.1021/acs.analchem.5b00147
*Anal. Chem.* 2015, 87, 5232−5239

**Table 2. Composition of Validation Samples and Predictions by Applying PARAFAC**

| | dibenzopyrene isomer (ng·mL$^{-1}$) | | | | | | | | | | | | | | |
|---|---|---|---|---|---|---|---|---|---|---|---|---|---|---|---|
| | DB[*a,e*]P | | | DB[*a,h*]P | | | DB[*a,i*]P | | | DB[*a,l*]P | | | N[2,3-*a*]P | | |
| sample | nom. | pred. | error (%) | nom. | pred. | error (%) | nom. | pred. | error (%) | nom. | pred. | error (%) | nom. | pred. | error (%) |
| V1 | 750 | 747 | −0.4 | 60 | 63 | 5.0 | 60 | 65 | 8.3 | 60 | 64 | 6.7 | 60 | 63 | 5.0 |
| V2 | 450 | 442 | −1.8 | 180 | 169 | −6.1 | 180 | 169 | −6.1 | 180 | 185 | 2.8 | 260 | 250 | −3.8 |
| V3 | 750 | 725 | −3.3 | 60 | 50 | −16.7 | 320 | 299 | −6.6 | 60 | 59 | −1.7 | 480 | 464 | −3.3 |
| V4 | 750 | 763 | 1.7 | 280 | 265 | −5.4 | 320 | 335 | 4.7 | 320 | 330 | 3.1 | 480 | 511 | 6.5 |
| V5 | 150 | 147 | −2.0 | 60 | 52 | −13.3 | 60 | 56 | −6.7 | 320 | 312 | −2.5 | 480 | 457 | −4.8 |
| V6 | 150 | 153 | 2.0 | 60 | 63 | 5.0 | 320 | 343 | 7.2 | 320 | 325 | 1.6 | 60 | 60 | 0.0 |
| V7 | 750 | 769 | 2.5 | 280 | 302 | 7.9 | 60 | 66 | 10.0 | 320 | 318 | −0.6 | 60 | 71 | 18.3 |
| V8 | 150 | 160 | 6.7 | 280 | 270 | −3.6 | 60 | 57 | −5.0 | 60 | 65 | 8.3 | 480 | 495 | 3.1 |
| V9 | 450 | 474 | 5.3 | 180 | 193 | 7.2 | 180 | 201 | 11.7 | 180 | 190 | 5.6 | 260 | 274 | 5.4 |
| V10 | 450 | 416 | −7.6 | 100 | 95 | −5.0 | 180 | 163 | −9.4 | 180 | 188 | 4.4 | 260 | 235 | −9.6 |
| V11 | 450 | 485 | 7.8 | 180 | 205 | 13.9 | 180 | 201 | 11.7 | 180 | 184 | 2.2 | 260 | 283 | 8.8 |
| V12 | 150 | 141 | −6.0 | 280 | 277 | −1.1 | 320 | 306 | −4.4 | 60 | 62 | 3.3 | 60 | 55 | −8.3 |
| REP (%)[a] | – | 4.2 | – | – | 7.6 | – | – | 8.1 | – | – | 3.3 | – | – | 6.5 | – |
| recovery (%) | – | 100.4 | – | – | 99.0 | – | – | 101.3 | – | – | 102.8 | – | – | 101.4 | – |

[a]REP (%) = 100 × $(((\Sigma_{i=1}^{I}(y_{pred} - y_{nom})^2)/I)^{1/2}/(y_{cal}))$, where $y_{pred}$ is the predicted concentration for the $i$th validation sample, $y_{nom}$ is the nominal concentration, $I$ is the number of validation samples, and $y_{cal}$ is the average of the nominal concentration values of the calibration set samples (450, 167, 187, 187, and 267 ppb, respectively).

**Table 3. Composition of Coal Tar Samples Spiked with the Five Targeted Isomers and PARAFAC Predictions**

| | dibenzopyrene isomer (ng·mL$^{-1}$)[a] | | | | | | | | | |
|---|---|---|---|---|---|---|---|---|---|---|
| | DB[*a,e*]P | | DB[*a,h*]P | | DB[*a,i*]P | | DB[*a,l*]P | | N[2,3-*a*]P | |
| coal-tar sample | nom. | pred. | nom. | pred. | nom. | pred. | nom. | pred. | nom. | pred. |
| original coal-tar sample[b] | 21 | 25 | 6 | 7 | 9 | 12 | 3 | – | 10 | 12 |
| spiked test sample #1 | 150 | 135 | 60 | 55 | 60 | 61 | 320 | 335 | 480 | 452 |
| spiked test sample #2 | 150 | 159 | 60 | 62 | 320 | 315 | 320 | 310 | 60 | 51 |
| spiked test sample #3 | 450 | 475 | 180 | 191 | 180 | 192 | 180 | 189 | 260 | 245 |
| spiked test sample #4 | 150 | 165 | 280 | 269 | 320 | 305 | 60 | 70 | 60 | 71 |
| REP (%)[c] | – | 7.6 | – | 5.7 | – | 4.5 | – | 5.1 | – | 8.1 |
| recovery (%) | – | 102.9 | – | 99.3 | – | 100.5 | – | 105.8 | – | 97.9 |

[a]nom. = nominal concentration; pred. = predicted concentration. All concentrations in ng·mL$^{-1}$. [b]Coal tar extract was diluted with *n*-octane, 1:375 (v/v). [c]REP (%) = 100 × $(((\Sigma_{i=1}^{I}(y_{pred}-y_{nom})^2)/I)^{1/2}/(y_{cal}))$, where $y_{pred}$ is the predicted concentration for the $i$th validation sample, $y_{nom}$ is the nominal concentration, $I$ is the number of validation samples, and $y_{cal}$ is the average of the nominal concentration values of the calibration set samples.

emission wavelengths of each PAH. The standard deviations of the blank signals did not change much with lowering the temperature to 4.2 K. The better LODs resulted from the steeper slopes of the calibration curves at liquid nitrogen and helium temperatures.

Figure 2 superposes the 4.2 K EEMs recorded from calibration samples of the five dibenzopyrene isomers. Figure 3A depicts the 4.2 K EEMs recorded from a validation sample of the five PAHs. Visual comparison of Figures 2 and 3A leads to at least one pair of excitation ($\lambda_{exc}$) and emission ($\lambda_{em}$) wavelengths that is free from the spectral interference of the other four isomers. This condition is met at the excitation and emission maxima of DB[*a,l*]P ($\lambda_{exc}/\lambda_{em}$ = 320/417 nm) and DB[*a,e*]P ($\lambda_{exc}/\lambda_{em}$ = 305/395 nm). Their determination in a synthetic mixture of the five isomers should then be possible at the concentration levels reported in Table S2, Supporting Information. However, for DB[*a,i*]P, DB[*a,h*]P, and N[2,3-*a*]P, wavelengths free of spectral overlapping are found away from the excitation and emission maxima. Table 1 reports the AFOM of these isomers at excitation and emission wavelengths free from spectral overlapping. Although the LODs are worse than those in Table S2, Supporting Information, the direct determination of DB[*a,i*]P, DB[*a,h*]P, and N[2,3-*a*]P in a synthetic mixture of the five isomers would still be possible at the parts-per-billion concentration level. As shown in Figure 3B, the presence of unknown fluorescence concomitants in the coal-tar sample leads to strong spectral overlapping within the entire EEM range of excitation and emission wavelengths. The direct determination of the five targeted isomers would not be possible without the aid of chemometrics.

**Validation and Test Set Results Obtained by PARAFAC Modeling.** The theory of PARAFAC has been extensively discussed in previous articles.[38] Only a brief description, which is directly related to fluorescence EEM data formats, will be provided here. A cube ($\boldsymbol{X}$) is built by stacking the matrices data of size ($J \times K$) corresponding to $I$ standards plus the sample data. Then, a trilinear decomposition, according to eq 1, is carried out to retrieve the values of $a_{in}$, $b_{jn}$, and $c_{kn}$ from a fitting procedure of the values of the elements $x_{ijk}$:

$$x_{ijk} = \sum_{n=1}^{N} a_{in} b_{jn} c_{kn} + e_{ijk} \quad (1)$$



DOI: 10.1021/acs.analchem.5b00147
*Anal. Chem.* 2015, 87, 5232−5239

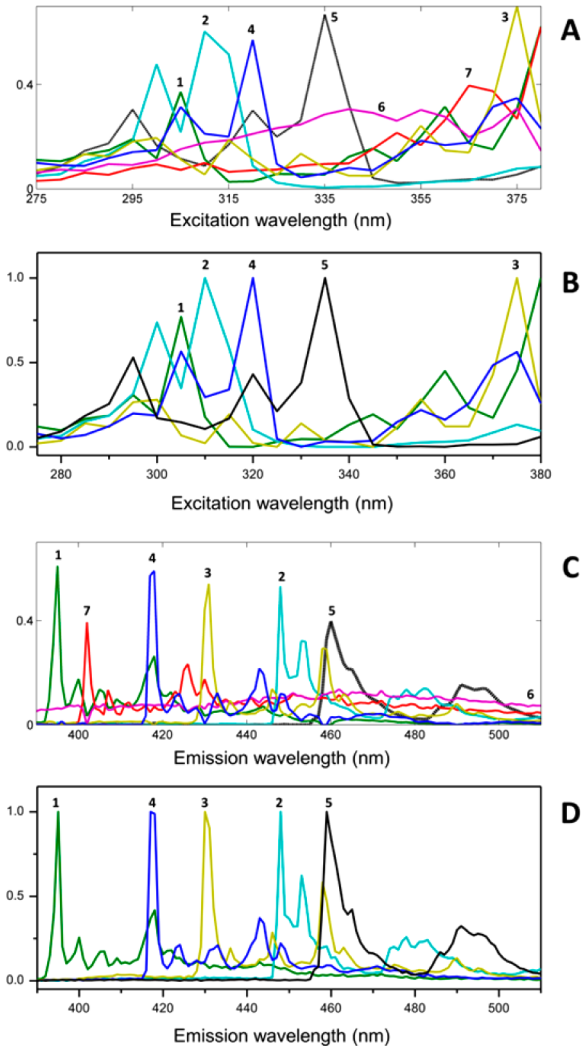


**Figure 4.** Excitation (A) and emission (C) profiles extracted with PARAFAC when analyzing a coal-tar sample (test sample #1, Table 3) spiked with the five targeted isomers; lines: 1 = DB[*a,e*]P, 2 = DB[*a,h*]P, 3 = DB[*a,i*]P, 4 = DB[*a,l*]P, 5 = N[2,3-*a*]P, and 6 = background; red line 7 corresponds to an unexpected component present in the coal-tar sample. (B) Excitation and (D) emission spectra recorded with the spectrofluorimeter from calibration samples of the five targeted isomers at 4.2 K. Spectra were recorded with the cryogenic fiber-optic probe using a 1 nm/1 nm excitation/emission band-pass. 1 = 200 ng·mL$^{-1}$ DB[*a,e*]P, 2 = 200 ng·mL$^{-1}$ DB[*a,h*]P, 3 = 200 ng·mL$^{-1}$ DB[*a,i*]P, 4 = 200 ng·mL$^{-1}$ DB[*a,l*]P, and 5 = 250 ng·mL$^{-1}$ N[2,3-*a*]P.

where $a_{in}$ denotes the values of the profile in the sample mode for constituent $n$ in sample $i$ (quantitative information); $b_{jn}$ and $c_{kn}$ are the corresponding profile values in both instrumental data modes for constituent $n$ (qualitative information); and $e_{ijk}$ collects the model errors, which are often unavoidable in experimental signals that carry noise. If $a_{in}$, $b_{jn}$, and $c_{kn}$ can be reliably obtained, it is customary to arrange them into three matrices: the matrix of *scores* **A** of size $[(I + 1 \times N)]$, containing all $a_{in}$ values, and the two matrices of *loadings* **B** (emission profiles of size $J \times N$, containing all $b_{jn}$ values) and **C** (excitation profiles of size $K \times N$, containing all $c_{kn}$ values).

In order to exploit the second-order advantage of three-way data, PARAFAC was separately applied to cubes of data formed by the EEMs recorded from (a) the 25 calibration samples (i.e., 5 standards per dibenzopyrene isomer) and (b) each one of the validation samples (V1−V12) in Table 2 or (c) the test samples in Table 3. The size of each of the cubes submitted to PARAFAC analysis was then 26 × 161 × 22; i.e., $(I + 1) \times J \times K$. The number of spectral components in each of the cubes ($N$) was obtained via core consistency analysis.[39] When analyzing the validation samples, $N$ was equal to 6, one spectrum per each of the studied isomers and one for the background signal. When analyzing coal tar samples with and without the addition of the five isomers, $N$ was equal to 7. This higher value indicates that an additional profile from an unexpected sample concomitant was retrieved by the PARAFAC modeling and informs us that the second-order advantage should be exploited.

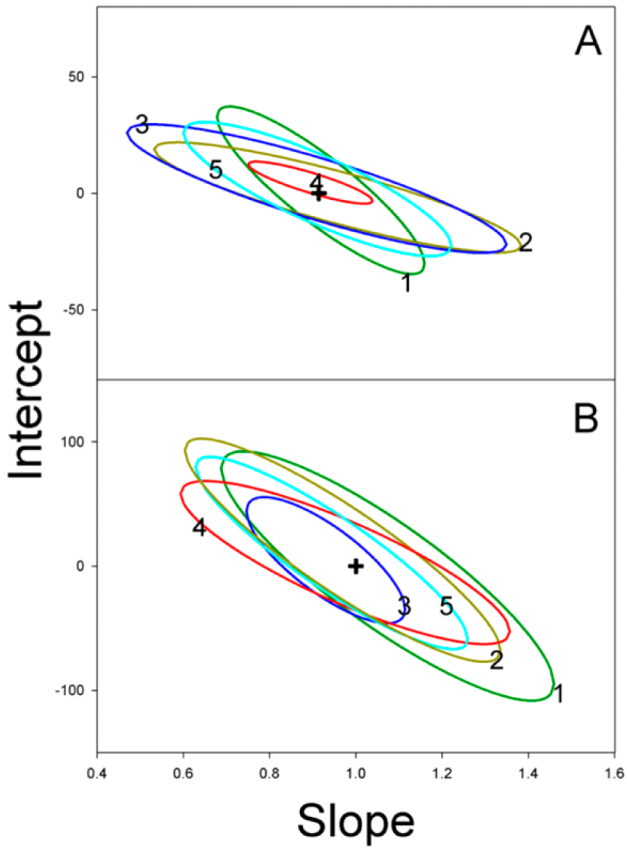


**Figure 5.** Elliptic joint confidence regions of PARAFAC predictions on (A) validation samples and (B) spiked coal-tar test samples. Solid lines: 1 = DB[*a,e*]P, 2 = DB[*a,h*]P, 3 = DB[*a,i*]P, 4 = DB[*a,l*]P, and 5 = N[2,3-*a*]P.

Figure 4 compares the excitation and emission spectra recorded from calibration samples to the loading matrices **B** and **C** obtained from PARAFAC when processing the spiked coal tar sample #1 and the set of calibration samples. Peak assignments 1−5 in the loading matrices were made based on the similarities of spectral profiles and maximum wavelengths of excitation and emission. Peak 6 was attributed to the background signal and peak 7 to an unexpected sample component that could interfere in the absence of the second order advantage.

Tables 2 and 3 summarize the prediction results for both sets samples. Due to the high complexity of the coal-tar sample, the REP% values and the recoveries of the five targeted isomers can be considered satisfactory. A statistical comparison of the prediction results was made via the bivariate least-squares


DOI: 10.1021/acs.analchem.5b00147
*Anal. Chem.* 2015, 87, 5232−5239

(BLS) regression method and the elliptic joint confidence region (EJCR) test.[40] The EJRC plots of the slopes and the intercepts are shown in Figure 5. The elliptical domains obtained for the five isomers in both sets of samples include the theoretically predicted value of the slope (1) and the intercept (0). This fact excludes the possible presence of biases in PARAFAC and demonstrates comparable precision and accuracy when analyzing samples with and without unexpected sample components.

**Limits of Detection and Limits of Quantitation Based on EEM/PARAFAC Analysis.** The LODs and LOQs obtained via multiway calibration were calculated with the aid of the general sensitivity (SEN) expression reported by Olivieri:[41]

$$\mathrm{SEN} = s_n\{\boldsymbol{\delta}_n^{\mathrm{T}}[\mathbf{Z}_{\mathrm{cal}}^{\mathrm{T}}(\mathbf{I} - \mathbf{Z}_{\mathrm{unx}}\mathbf{Z}_{\mathrm{unx}}{}^{+})\mathbf{Z}_{\mathrm{cal}}]^{-1}\boldsymbol{\delta}_n\}^{-1/2} \quad (2)$$

where $s_n$ is the slope of the PARAFAC pseudounivariate plot, $\boldsymbol{\delta}_n$ is a column vector of size $N_{\mathrm{cal}} \times 1$ with zeros except for a "1" in the position of the analyte of interest, $\mathbf{Z}_{\mathrm{cal}}$ is the Khatri-Rao product of the matrices containing the profiles in both modes for the calibrated components ($\mathbf{C}_{\mathrm{cal}}$ and $\mathbf{B}_{\mathrm{cal}}$), and $\mathbf{Z}_{\mathrm{unx}}$ contains profiles in both modes for the unexpected components.

Considering a 95% confidence level for Type I ($\alpha = 0.05$) and II errors ($\beta = 0.05$) and assuming that the Gaussian curves in the absence and the presence of analyte have identical widths, the LOD and the LOQ can be calculated as $3.3 \times s_0$ and $10 \times s_0$, respectively. The term $s_0$, which corresponds to the uncertainty prediction of the background sample, is computed with eq 3:

$$s_0 = [\mathrm{SEN}^{-2}\sigma_x{}^2 + h_0\mathrm{SEN}^{-2}\sigma_x{}^2 + h_0\sigma_{y\mathrm{cal}}{}^2] \quad (3)$$

where $h_0$ is the leverage for a blank sample and $\sigma_x$ and $\sigma_{y\mathrm{cal}}$ are the uncertainties in signal and calibration concentration, respectively. For the five studied isomers, the LOD/LOQ values were the following ($\mathrm{ng \cdot mL^{-1}}$): D[*a*,*l*]P = 0.40/1.21, D[*a*,*i*]P = 0.11/0.33, D[*a*,*h*]P = 0.22/0.67, N[2,3-*a*]P = 0.31/0.94, and D[*a*,*e*]P = 1.51/4.58. The comparison of these values to those reported in Table S2, Supporting Information, show LOD improvements in all cases. This is in good agreement with previous reports showing LOD improvements when going from a one-way to a three-way calibration method.[38]

## CONCLUSIONS

A novel method for the direct determination, i.e., without chromatographic separation, of DB[*a*,*l*]P, DB[*a*,*h*]P, DB[*a*,*i*]P, DB[*a*,*e*]P, and N[2,3-*a*]P in coal-tar samples has been developed on the basis of the collection of 4.2 K EEM and data processing with PARAFAC. Easy collection of steady-state EEM was accomplished with the aid of a cryogenic FOP and commercial instrumentation. Lowering the temperature to 4.2 K provided sufficient spectral narrowing for the accurate determination of the five dibenzopyrene isomers via PARAFAC at parts-per-billion concentration levels. The simplicity and the environmentally friendly nature of the experimental procedure, associated with the excellent analytical figures of merit, provide a valuable alternative for screening these highly toxic HMW-PAHs in coal-tar samples.

## ASSOCIATED CONTENT

### Supporting Information

Additional data available as noted in the text. The Supporting Information is available free of charge on the ACS Publications website at DOI: 10.1021/acs.analchem.5b00147.

## AUTHOR INFORMATION


### Corresponding Author

*E-mail: Andres.campiglia@ucf.edu. Fax: +1 407 823 2252.


### Notes

The authors declare no competing financial interest.

## ACKNOWLEDGMENTS


The authors thank Dr. Stephen A. Wise of the National Institute of Standards and Technology (NIST) for providing the standard reference material. Dr. Goicoechea is grateful to Universidad Nacional del Litoral (Project CAI+D 2012 No. 11-11), to CONICET (Consejo Nacional de Investigaciones Científicas y Técnicas, Project PIP 455), and to ANPCyT (Agencia Nacional de Promoción Científica y Tecnológica, Project PICT 2011-0005) for financial support. Dr. Fernando Barbosa Jr. is grateful to Conselho Nacional de Desenvolvimento Científico e Tecnológico (CNPq) and Fundação de Amparo à Pesquisa do Estado de São Paulo (FAPESP) (Projects 2012/03465-1 and 2014/00986-6) for financial support.


## REFERENCES


(1) Kobayashi, R.; Okamoto, R. A.; Maddalena, R. A.; Kado, N. Y. *Environ. Res.* **2008**, *107*, 145−151.
(2) Courter, L. A.; Luch, A.; Tamara, M. J.; Arlt, V. M.; Fischer, K.; Bildfell, R.; Pereira, C.; Phillips, D. H.; Poirier, M. C.; Baird, W. M. *Cancer Lett.* **2008**, *265*, 135−147.
(3) Lin, C.-C.; Chen, S.-J.; Huang, K.-L.; Lee, W.-J.; Lin, W.-Y.; Tsai, J.-H.; Chaung, H.-C. *Environ. Sci. Technol.* **2008**, *42*, 4229−4235.
(4) Park, J. H.; Gelhaus, S.; Vedantam, S.; Oliva, A. L.; Batra, A.; Blair, I. A.; Troxel, A. B.; Field, J.; Penning, T. M. *Chem. Res. Toxicol.* **2008**, *21*, 1039−1049.
(5) U.S. Environmental Protection Agency, Drinking Water Standards; http://www.epa.gov/safewater/standards.html.
(6) Castro, D.; Slezakova, K.; Delerue-Matos, C.; Alvim-Ferraz, M. C.; Morais, S.; Pereira, M. C. *Atmos. Environ.* **2011**, *45*, 1799−1808.
(7) Lauer, F. T.; Walker, M. K.; Burchiel, S. W. *J. Toxicol. Environ. Health, Part A* **2013**, *76*, 16−24.
(8) Rodríguez, F. A.; Liu, Z.; Lin, C. H.; Ding, S.; Cai, Y.; Kolbanovskiy, A.; Kolbanovskiy, M.; Amin, S.; Broyde, S.; Geacintov, N. E. *Biochemistry* **2014**, *53*, 1827−1841.
(9) Madeen, E.; Corley, R. A.; Crowell, S.; Turteltaub, K.; Ognibene, T.; Malfatti, M.; McQuistan, T. J.; Garrard, M.; Sudakin, D.; Williams, D. E. *Chem. Res. Toxicol.* **2015**, *28*, 126−134.
(10) Wilson, W. B.; Campiglia, A. D. *J. Chromatogr. A* **2011**, *1218*, 6922−6929.
(11) Cavalerie, E. L.; Higginbotham, S.; RamaKrishna, N. V. S.; Devanesan, P. D.; Todorovic, R.; Rogan, E. G.; Salmasi, S. *Carcinogensis* **1991**, *12*, 1939−1944.
(12) Devanesan, P.; Ariese, F.; Jankowiak, R.; Small, G. J.; Rogan, E. G.; Cavalieri, E. L. *Chem. Res. Toxicol.* **1999**, *12*, 789−795.
(13) Mumford, J. L.; Harris, D. B.; Williams, K.; Chuang, J. C.; Cooke, M. *Environ. Sci. Technol.* **1987**, *21*, 308−311.
(14) Nahorniak, M. L.; Booksh, K. S. *Analyst* **2006**, *131*, 1308−1315.
(15) Bortolato, S. A.; Arancibia, J. A.; Escandar, G. M. *Anal. Chem.* **2008**, *80*, 8276−8286.
(16) Bortolato, S. A.; Arancibia, J. A.; Escandar, G. M. *Environ. Sci. Technol.* **2011**, *45*, 1513−1520.
(17) Huang, L.; Chernyak, S. M.; Batterman, S. A. *Sci. Total Environ.* **2014**, *487*, 173−186.
(18) Van Metre, P. C.; Mahler, B. J. *Environ. Sci. Technol.* **2014**, *48*, 7222−7228.
(19) Mahler, B. J.; Van Metre, P. C.; Foreman, W. T. *Environ. Pollut.* **2014**, *188*, 81−87.
(20) Williams, E. S.; Mahler, B. J.; Van Metre, P. C. *Environ. Sci. Technol.* **2013**, *47*, 1101−1109.




DOI: 10.1021/acs.analchem.5b00147
*Anal. Chem.* 2015, 87, 5232−5239

(21) Kozin, I. S.; Gooijer, C.; Velthorst, N. H. *Anal. Chem.* **1995**, *67*, 1623−1626.
(22) Kozin, I. S.; Gooijer, C.; Velthorst, N. H.; Harmsen, J.; Wieggers, R. *Int. J. Environ. Anal. Chem.* **1995**, *61*, 285−297.
(23) Colmsjo, A. L.; Wise, S. A. *Anal. Chim. Acta* **1986**, *187*, 129−137.
(24) Wise, S. A.; Benner, B. A.; Liu, H.; Byrd, G. D.; Colmsjoe, A. *Anal. Chem.* **1988**, *60*, 630−637.
(25) Schubert, P.; Schantz, M. M.; Sander, L. C.; Wise, S. A. *Anal. Chem.* **2003**, *75*, 234−246.
(26) Bergvall, C.; Westerholm, R. *Environ. Sci. Technol.* **2007**, *41*, 731−737.
(27) Bergvall, C.; Westerholm, R. *Anal. Bioanal. Chem.* **2008**, *391*, 2235−2248.
(28) Yu, S. J.; Campiglia, A. D. *Appl. Spectrosc.* **2004**, *58*, 1385−1393.
(29) Yu, S. J.; Campiglia, A. D. *Anal. Chem.* **2005**, *77*, 1440−1447.
(30) Wilson, W. B.; Campiglia, A. D. *Analyst* **2011**, *136*, 3366−3374.
(31) Wang, H. Y.; Yu, S. J.; Campiglia, A. D. *Anal. Biochem.* **2009**, *385*, 249−256.
(32) Bystol, A. J.; Thorstenson, T.; Campiglia, A. D. *Environ. Sci. Technol.* **2002**, *36*, 4424−4429.
(33) Campiglia, A. D.; Bystol, A. J.; Yu, S. J. *Anal. Chem.* **2006**, *78*, 484−492.
(34) Moore, A. F. T.; Barbosa, F.; Campiglia, A. D. *Appl. Spectrosc.* **2014**, *68*, 14−25.
(35) Olivieri, A. C.; Wu, H.-L.; Yu, R.-Q. *Chemom. Intell. Lab. Syst.* **2009**, *96*, 246−251.
(36) www.iquir-conicet.gov.ar/descargas/mvc2.rar.
(37) Miller, J. N.; Miller, J. C. *Statistics and Chemometrics for Analytical Chemistry*, 4th ed.; Prentice-Hall: New York, 2000.
(38) Escandar, G. M.; Goicoechea, H. C.; Muñoz de la Peña, A.; Olivieri, A. C. *Anal. Chim. Acta* **2014**, *806*, 8−26.
(39) Bro, R.; Kiers, H. A. L. *J. Chemom.* **2003**, *17*, 274−286.
(40) Riu, J.; Rius, F. X. *TrAC, Trends Anal. Chem.* **1997**, *16*, 211−216.
(41) Olivieri, A. C. *Anal. Chem.* **2005**, *77*, 4936−4946.



DOI: 10.1021/acs.analchem.5b00147
*Anal. Chem.* 2015, 87, 5232−5239